Return to previous file: Streamshade01.pdf

Community metabolism

The influence of shade on photosynthetic rate was examined by fitting to the measurements a photosynthesis-irradiance (P-I) model with no photoinhibition (Webb *et al.* 1974). Although there was a suggestion of photoinhibition in some P-I plots at high irradiances, the photoinhibition model of Platt *et al.* (1980) often produced unrealistic coefficient values and high error terms. The Webb model used is:

$$P = P_{max}\,(1 - exp(-\frac{I}{I_k})) \qquad 3$$

where I = irradiance (μE m^{-2} s^{-1}), P_{max} = biomass specific maximum (i.e., light saturated) photosynthesis rate (mg(carbon) mg^{-1}(Chl. *a*) $hour^{-1}$) and I_k = irradiance at which P = 0.632 P_{max} (μE m^{-2} s^{-1}). α = initial slope of the P-I curve (mg C mg^{-1}(Chl. *a*) $hour^{-1}$ (μE m^{-2} $s^{-1})^{-1}$) (α = P_{max}/I_k). This model was fitted to the data using Kaleidagraph, which employs the Levenberg-Marquardt algorithm (Press *et al.* 1986). An example curve fit is presented in Fig**.** 22. A summary of best-fit parameter values for each treatment is given in Table 7.

Chlorophyll-specific photosynthetic capacity (P_{max}) and initial slope (α) were both highly variable within treatment and showed no clear dependence on shade. However, the irradiance level at which light saturation of photosynthesis occurred (I_k) was lowest in the high shade treatments, indicating some degree of shade adaption by the periphyton. Both chlorophyll-specific P_{max} and α showed a negative correlation with biomass (Fig. 23), which suggests self-shading within the biofilm.

Table 7 Mean and standard error values of coefficients in the photosynthesis-irradiance equation

% Shade	P_{max} (mgC mg^{-1}Chl. *a* h^{-1})	I_k μE m^{-2} s^{-1}	P_{max}/I_k
0	6.2 ± 3.7	311 ± 130	29 ± 24
60	9.1 ± 0.9	112 ± 31	103 ± 40
90	5.8 ± 0.6	65 ± 10	97 ± 25
98	3.7 ± 0.1	72 ± 7	52 ± 4

Figure 22 An example of measured photosynthesis-irradiance response (circles) and Equation 3 (line).

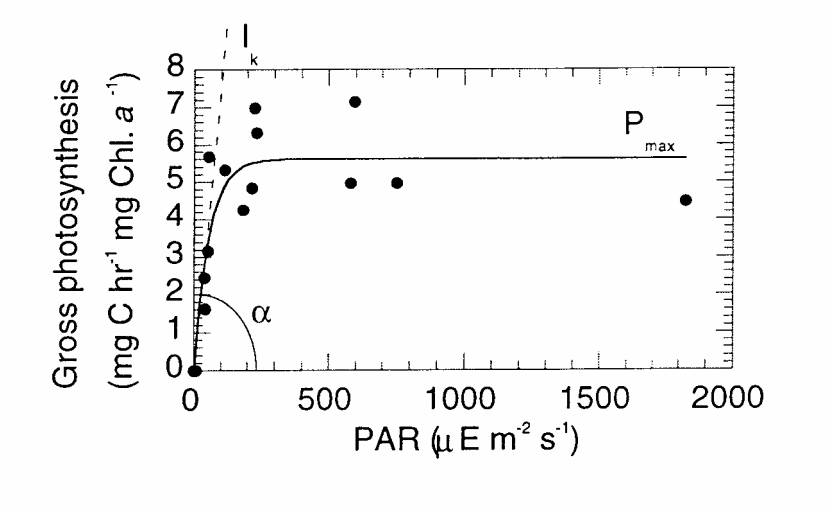

Figure 23 Relationships between periphyton biomass and chlorophyll-specific photosynthetic capacity (P_{max}) and efficiency (α) as a function of %shade.

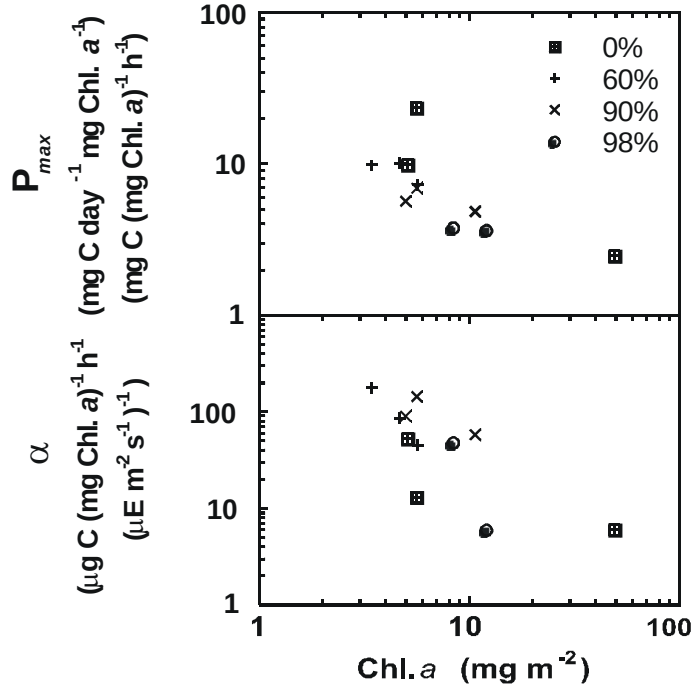

Figure 24 Time series of gross carbon fixation rate estimated from measured PAR using the fitted P-I relationships for each shade treatment.

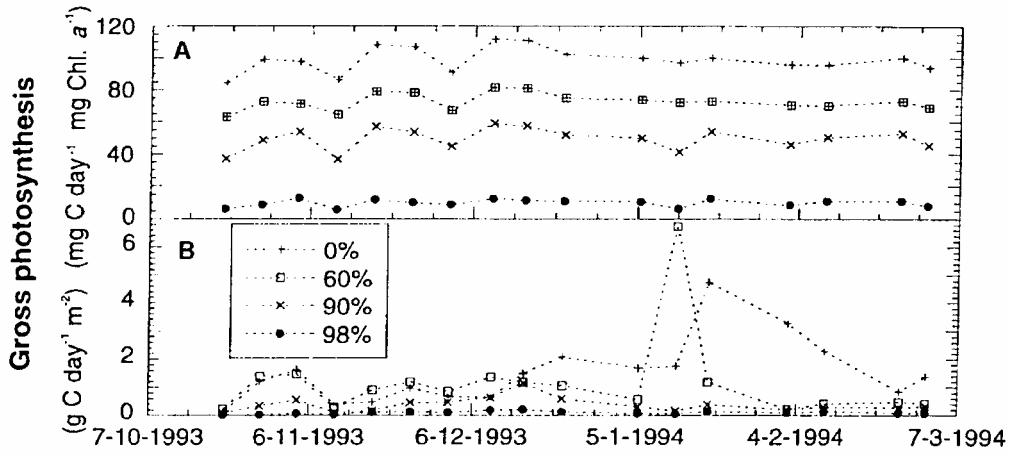

Daily primary productivity (carbon fixation) was estimated by combining the fitted P-I curves with the daily PAR record. Because irradiance in the 90% and 98% treatments falls below the level required for saturation of photosynthesis (I_k) for at least part of the day, daily chlorophyll-specific productivity is strongly influenced by shade (Fig. 24) (i.e., gross photosynthesis per unit of chlorophyll is markedly lower). Area-specific productivity also shows an influence of shade treatment (Fig. 24) although the response is less marked because of the confounding influence of fluctuating biomass. Nevertheless, there is clear evidence that gross photosynthesis (per unit area) is markedly higher in the more open channels (0% and 60% treatments). Although considerably more carbon is fixed at lower shade, this is not reflected in biomass accrual, except for occasional 'blooms' (Fig. 21). The conclusion we draw is that, as primary productivity increases, the biomass is efficiently 'cropped' by grazing invertebrates.

Nitrogen uptakes rates (mg NO_3-N m^{-2} d^{-1}) were greatest in the open channels and declined with increasing shade (Fig. 25). Uptake rate was not significantly correlated with algal biomass ($r^2 = 0.1$), but was fairly strongly related to gross photosynthetic rate ($r^2 = 0.8$) as would be expected.

Figure 25 Measured nitrate uptake rates on five sampling dates as a function of % shade.

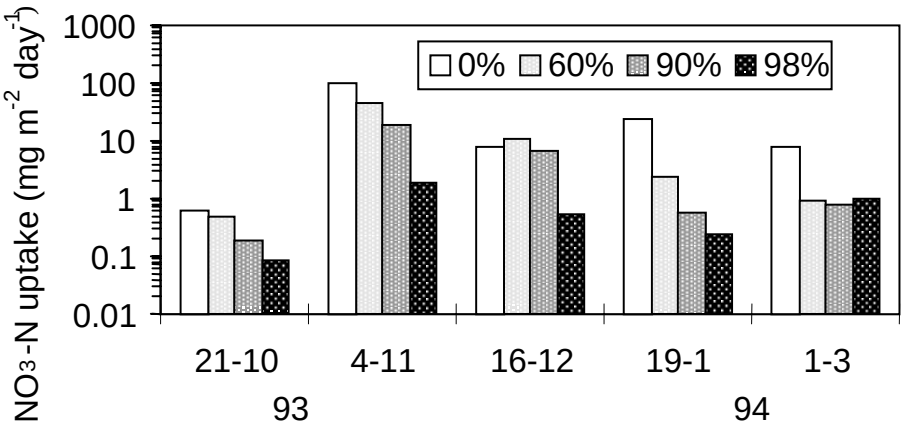

Invertebrate communities

The mean initial invertebrate density in the channel gravels (393 per 0.1 m^2) was fairly high, being approximately equal to the 80 percentile for the sites in the '100 rivers' study (Quinn & Hickey 1990). No significant differences were detected between shade treatments in terms of their initial taxonomic richness, total invertebrate density or the density of any individual taxon (ANOVA, $P > 0.05$). This indicates that differences which developed during the experiment are attributable to the shade manipulations. We have no way of knowing whether these differences were the result of immigration/emigration or birth/death.

Differences between channels in gravel invertebrate communities measured at the end of the experiment (142 days after the initial sampling) are shown in Fig. 26. The time-series of invertebrate abundance on the tiles exposed to contrasting shade during the main experiment are shown in Fig. 27 and those in the recolonisation experiment are shown in Fig. 28.

For almost all invertebrates the shade response measured in the tile and gravel experiments matched. The only exception was the collector-browser mayfly *Zephlebia*, which appeared to favour 90% shade in the gravel experiment but showed no preference in the tile experiment. Some invertebrates colonised the gravels but were not found in significant numbers on the tiles (notably oligochaetes) whereas the converse applied to some other invertebrates (notably *Austrosimulium*). The majority of invertebrates, however, were found in large enough numbers on both media to assess shade effects.

The abundance of several invertebrates decreased as shade increased. Some declined monotonically with shade, some showed changes between 60% and 90% shade, while some showed effects only at 98% shade. We will not attempt to describe or explain

these subtle differences in shade response. Rather we will highlight the major differences that appeared consistently in our three experiments.

Numbers of several invertebrates decreased significantly with increasing shade:

- chironomids,
- oligochaetes, and
- the collector-browser stonefly *Megaleptoperla.*

Several invertebrate species showed a weak decreasing trend with increasing shade:

- the grazing case-caddis *Pycnocentrodes*,
- the grazing case-caddis *Helicopsyche*,
- the grazing limpet *Latia*,
- the grazing (algal piercing) caddis *Oxyethira*, as did
- taxonomic richness, and
- total density (i.e. total number of individuals per unit area).

Two invertebrate species, both filter feeders, showed a distinct preference for shade:

- the caddis *Aoteapsyche*, and
- the sandfly *Austrosimulium*.

One invertebrate species appeared to be unaffected by shade:

- the case-caddis *Olinga*.

Several other invertebrate species showed no significant shade response, either because of high variability within replicates or an inconsistent response between experiments and/or treatments. Thus a definite shade response was not detected for:

- the grazing snail *Potamopyrgus*,
- the collector-browser mayfly *Deleatidium*,
- the collector-browser mayfly *Zephlebia*, and
- the collector-gatherer beetle larva *Elmidae.*

Figure 26 Shade treatment effects on taxonomic richness and benthic invertebrate density (per 0.1 m^2, mean ± SE) in the stream channel gravels at the end of the experiment. Taxa that differed significantly between shade treatments (one-way ANOVA, $P < 0.05$, n=3 per treatment) are denoted by an asterisk.

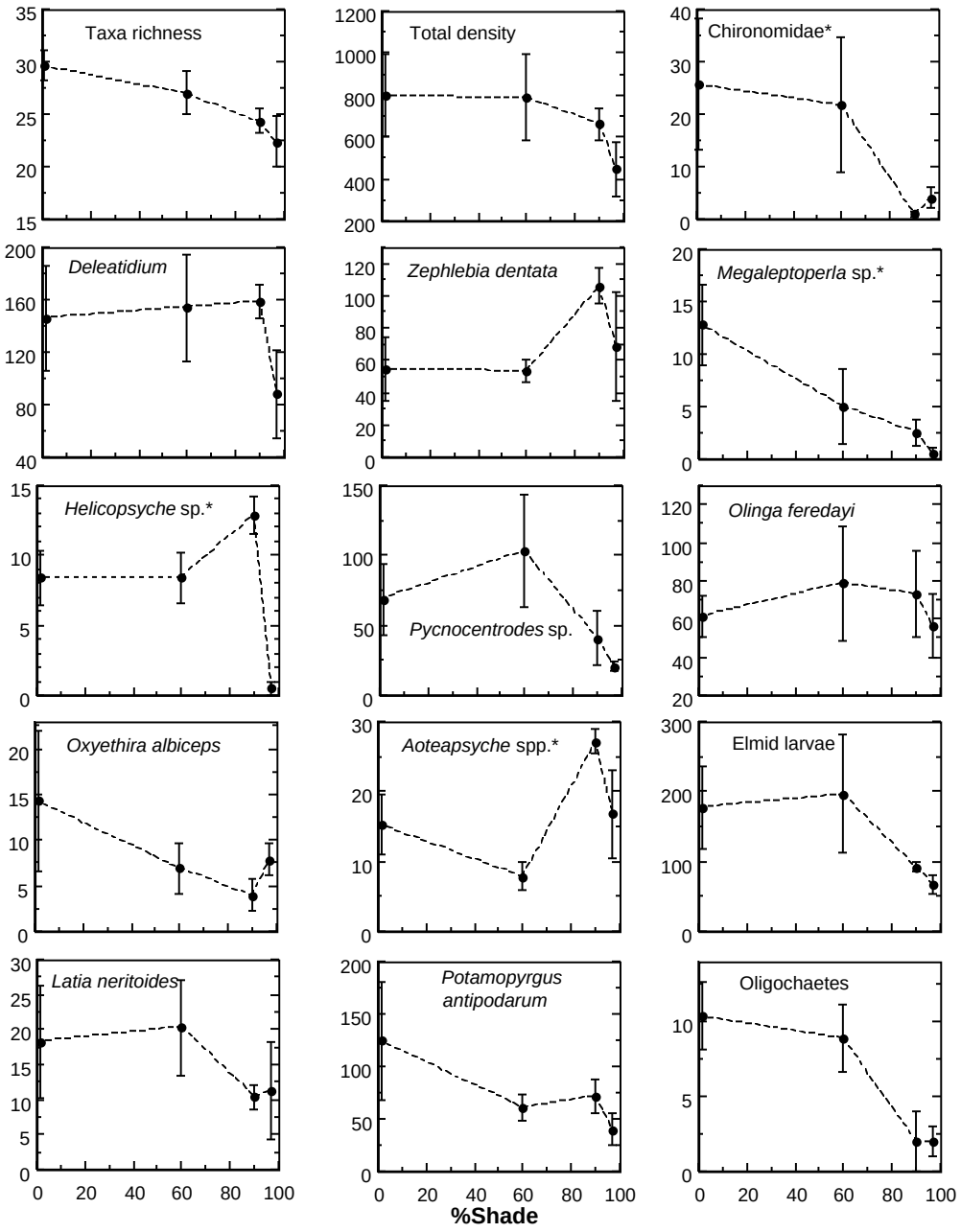

Figure 27 Taxonomic richness and benthic invertebrate density (per 0.1 m^2, mean ± SE) on the tiles during the main experiment under shade treatments of 0% (square), 60% (+), 90% (x) and 98% (circle). Treatments that did not differ significantly (nested ANOVA, post-hoc Scheffe test $P > 0.05$) are joined by an underline.

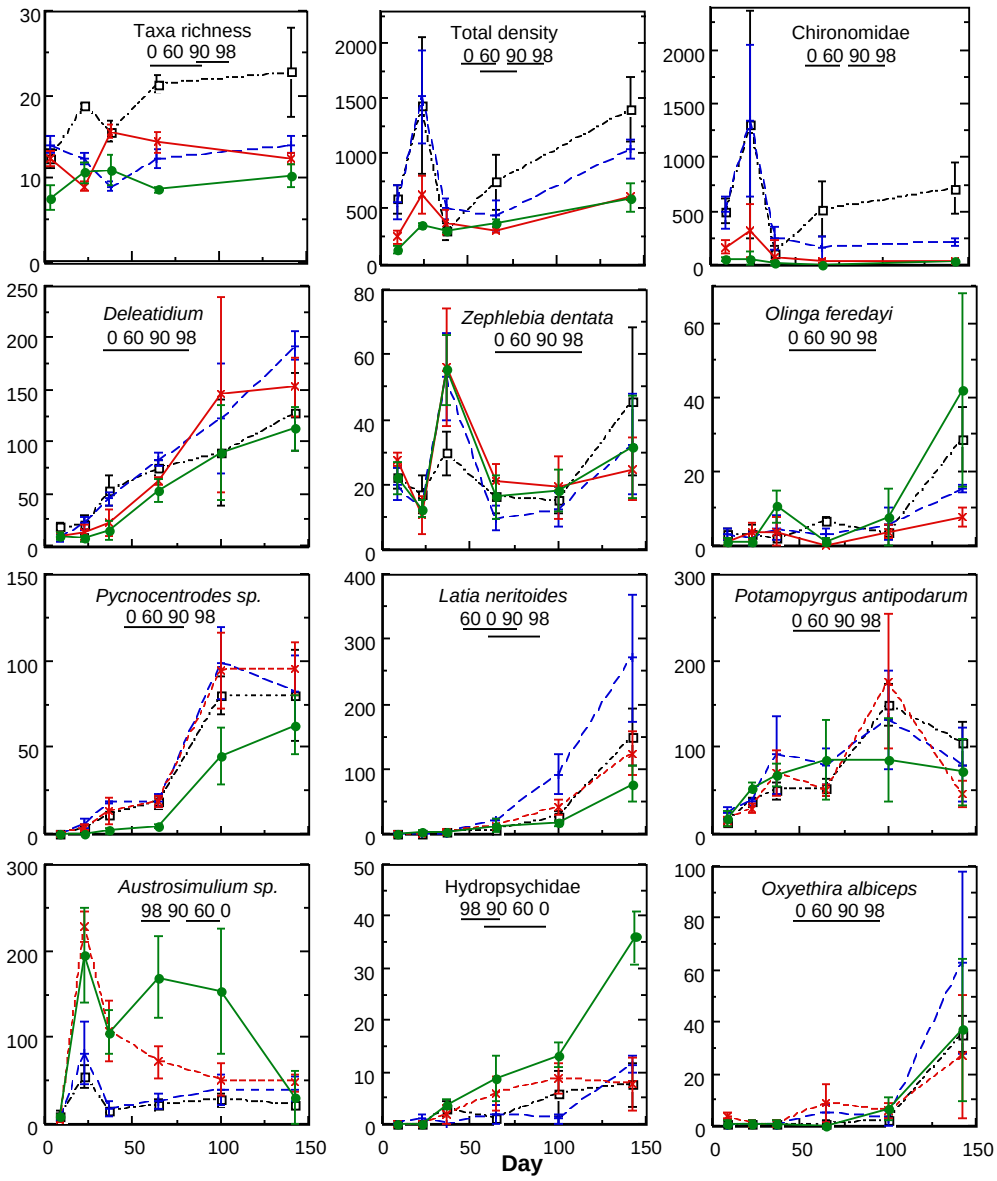

Figure 28 Taxonomic richness and benthic invertebrate density (per 0.1 m^2, mean ± SE) on the tiles during the summer recolonisation experiment under shade treatments of 0% (square), 60% (+), 90% (x) and 98% (circle). Treatments that did not differ significantly (nested ANOVA, post-hoc Scheffe test, $P > 0.05$) are joined by an underline.

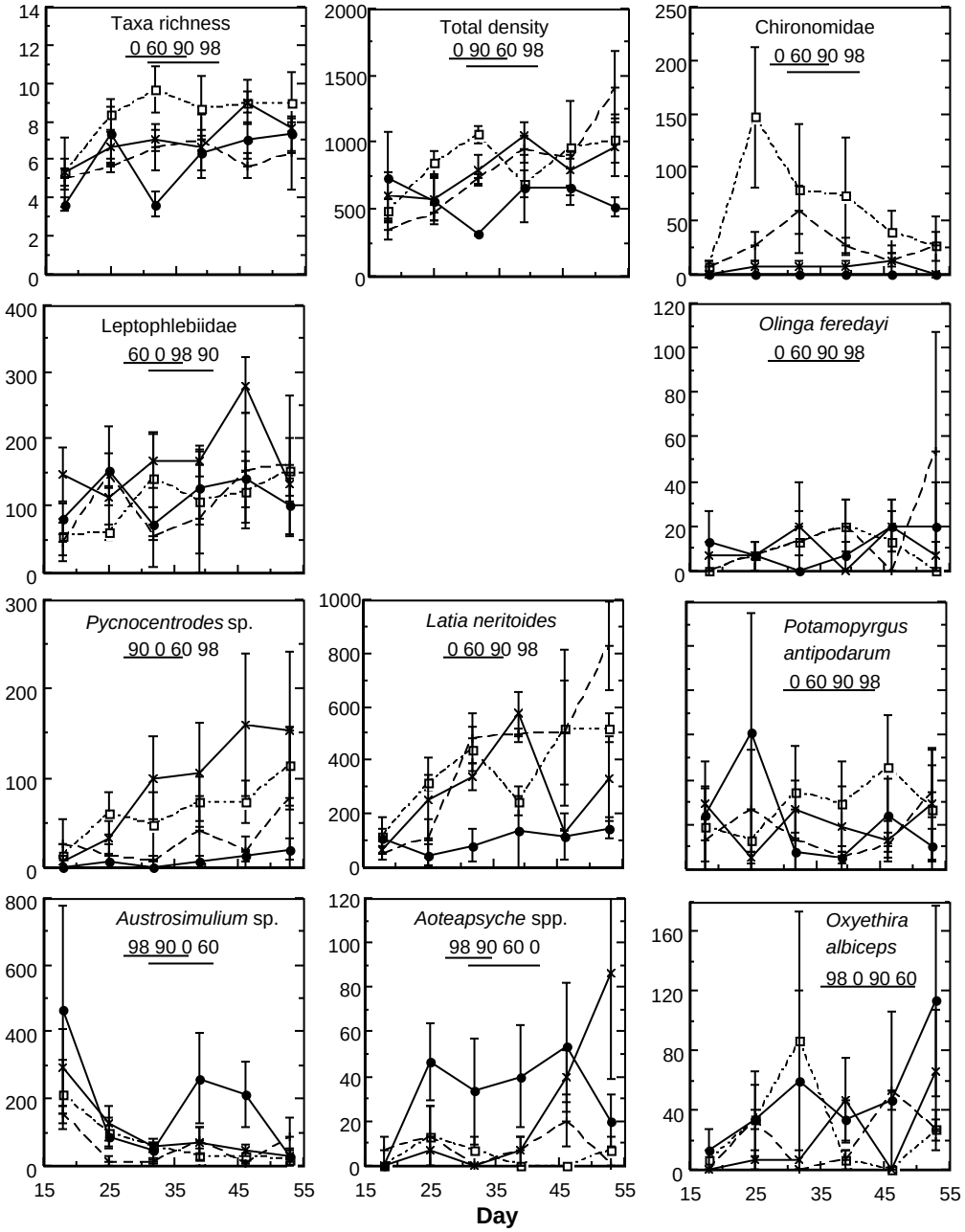

3.4 Discussion

Experimental design

Two aspects of our experimental design need to be considered when interpreting results and drawing implications for stream management: the spatial scale of the shade treatments, and the light quality.

Firstly, the shade treatments only affected small patches (area = 0.48 m^2) of an otherwise comparatively open pasture stream. The shade treatments did not alter the thermal regime or the supply to the channels from upstream of nutrients, dissolved particulate organic carbon, or drifting invertebrates; unlike changing riparian vegetation over a whole reach or catchment. Our shaded channels had a temperature regime very similar to the unshaded channels (i.e., the channels were too short for the lower radiation inputs to cause significant cooling). In reality, shaded streams are typically much cooler than unshaded streams (daily maximum temperatures in summer differ by up to 6ºC at Whatawhata, see Section 4). Organisms with low temperature tolerances could possibly be absent from our shaded channels, because they are absent from the warm pasture source stream, although found in shaded streams.

In our experimental channels the mass flux of dissolved and particulate carbon was determined by conditions in the source pasture stream (i.e., were unaffected by the shade manipulations). Natural riparian vegetation, however, provides an additional carbon source to shaded stream (viz., litterfall and woody debris), and hence an increased diversity of carbon sources is available to stream animals which may compensate for suppression of autotrophic production by shade. Restoration of riparian vegetation may also affect the supply of dissolved organic carbon, nutrients and sediment, which in turn may affect periphyton and heterotrophic biofilm communities.

Thus, our experiments help to identify the direct effects of reducing the light input to a short reach of the channel (e.g., by restoring riparian vegetation to a short reach but leaving the headwaters unshaded).

Secondly, unlike the black shade cloth used in our channel experiments (which is spectrally neutral) riparian vegetation alters both light quantity and quality. In Section 1 there is a brief discussion of the enrichment of visible light with green wavelengths as it passes through the canopy. The ecological implications of this change in light quality, however, have not been clearly established and this topic requires further investigation. We are inclined to the view that changes in the spectral composition of light have a markedly smaller ecological impact than the changes in the total amounts of radiation reaching streams. The remaining discussion is founded on this premise.

Periphyton

Our mesocosm experiment quantified several key responses of stream periphyton to manipulation of light inputs, in the absence of other factors which may be expected to co-vary with manipulation of riparian vegetation. Even though other physico-chemical conditions were favourable (e.g., nutrients and temperature) shading of 90% and 98% restricted biomass. The shade level of 98% is similar to that measured in headwater streams within forest catchments (see Sections 1 and 2) and our mesocosm results strongly suggest, therefore, that shading is the primary mechanism for restricting periphyton biomass in these streams. The consistently low periphyton biomass at 90% shade suggests that, to control periphyton in our headwater pasture streams, riparian plantings need to reduce light levels to about 10% of the total available light at an open site but do not need to be as densely shading as native bush (typically 98% shade). At shade levels of 0% and 60% it is clear that the potential exists for periphyton biomass to reach 'bloom' levels, albeit spasmodically. The minimum shade level required to control such blooms lies somewhere between 60% and 90% (i.e., 10–40% lighting).

In order to understand the observed responses of periphyton biomass to different light inputs it is necessary to look at the influence of shade on the balance between algal production and loss mechanisms. Periphyton productivity, as measured by daily carbon fixation rate per unit biomass, was lower at 90% and 98% shade than at 0% and 60% shade (Fig. 24) despite some shade adaptation (Table 7). We interpret the lack of significant biomass accrual in the 90% and 98% shade treatments to the ability of grazing invertebrates to consistently crop the carbon fixed at these low light levels. At 0% and 60% shade, such 'top-down' control was also effective for much of the time, but occasionally growth rate apparently outstripped grazing control. For each shade treatment, carbon fixation rates per unit biomass remained relatively constant throughout the experiment (Fig. 24), suggesting that the spasmodic nature of periphyton blooms was a consequence of periodic decreases in invertebrate grazing. Existing knowledge of factors controlling invertebrate grazing rates is scarce, and further research is required to elucidate the 'trigger' mechanism(s) by which periphyton are released from 'top-down' control. We note that, in our study, periphyton blooms did not occur until daily mean stream temperatures exceeded about 16–17ºC, and daily maximum temperatures exceeded about 20ºC. While lethal temperatures for stream invertebrates are above 22ºC (Quinn *et al.* 1994b), casual observation suggests that invertebrates show reduced activity at temperatures somewhat below those causing death. Thus, rising water temperature may be a potential 'trigger' factor. Controlled experiments that examine the interactions between light, periphyton, invertebrates and temperature are planned.

The similarity in algal community composition between the 60% and 90% and 98% shade treatments indicates that, while manipulation of light inputs influenced algal

biomass, it had only a minor influence upon algal community structure and pigment composition. The higher level of beta-carotene in the 0% shade treatment does suggest some adaptive response to high irradiance: beta-carotene is regarded as a major photo-protectant in algae (Ferris & Christian 1991). Our findings with spectrally-neutral shade cloth need to be treated with caution, as the effects may differ under natural shade.

As would be expected, we found nitrate-nitrogen uptake rates by periphyton to be correlated with carbon fixation rates. Our results indicate that the nutrient regime in pasture streams would be markedly altered by restoring riparian vegetation. Given the same nitrate input, a riparian shaded stream would act primarily as a downstream 'transporter' of nitrate. By comparison, an unshaded stream would act primarily as a 'processor' of this nitrate, converting nitrate to biomass and storing it in the channel under stable flow. Under high flows, much of the stored nitrogen may be flushed down stream in particulate form.

Invertebrates

Findings from our channel experiments accord well with our understanding of how stream ecosystems function, derived from the landuse comparisons (Section 2) and similar studies elsewhere. Table 8 compares the major shade responses shown by invertebrates in our channel experiments (Section 3) and landuse comparisons (Section 2).

In the channels, gross photosynthesis, and hence the rate of supply of autochthonous carbon to grazing invertebrates, declined with increasing shade. This is the most likely reason for the decline in abundance with increasing shade of the Chironomidae, *Pycnocentrodes*, and *Helicopsyche*: all are grazers whose primary food source is periphyton (notably diatoms). Evidence of invertebrate grazing activity in the experimental channels is afforded by the observation that the high carbon fixation rates calculated from our light and fixation measurements were not reflected in a commensurate accumulation in periphyton biomass. Even allowing for some loss by sloughing, there is clear evidence that grazing pressure was significant in the channels. The higher proportions of grazers (notably snails and chironomids) in open pasture streams than shaded forest streams is probably also a response to increased in-stream primary production.

The snail *Potamopyrgus*, surprisingly, responded only weakly to shade in the channel experiments. One possible reason is that *Potamopyrgus* utilises other food sources besides periphyton, notably heterotrophic biofilms (Rounick & Winterbourn 1983a). We did not quantify heterotrophic biofilm biomass or identify the food preferences of invertebrates in our channel experiments. However, we expect heterotrophic biofilm productivity to be unaffected by shade treatment, since the upstream supply of DOC

(which the biofilms utilise) was unaffected. If so then it seems probable that *Potamopyrgus* could maintain their population in the shaded channels by switching food sources from periphyton to heterotrophic biofilms. In the landuse comparisons, however, snails were significantly more abundant in the open pasture streams than in the shaded forest streams. It is not clear why snail populations responded to shade differently in the experimental channels and the landuse experiments.

Oligochaetes consume detrital material (CPOM and FPOM) associated with periphyton mats (either allochthonous material trapped within the mat or detrital carbon originating from in-stream production) and are known to tolerate low sediment or biofilm dissolved oxygen concentrations. Chironomids are either grazers or collector-browsers of detrital material and are also tolerant of organic enrichment. It is not surprising, therefore, that our channel and landuse comparison studies showed the biomass of these invertebrates increasing with increasing periphyton production (i.e., decreasing shade). Chironomids and oligochaetes made a significant contribution to both taxonomic richness and total density, and both groups declined significantly with increased shade.

Filter feeders would be expected to favour fairly 'clean' stream sediments (to provide attachment sites) and water to filter which is not high in inorganic suspensoids. The marked preference for shade shown by *Aoteapsyche* and *Austrosimulium* in our channel experiments indicates that abundant periphyton disadvantages these filter feeders. Periphyton may either coat stones, thereby preventing attachment, or overgrow filter feeders once they become attached, thereby reducing the flow of water and (hence the supply of food and oxygen). In the landuse comparison, two filter feeders (*Coloburiscus* and *Orthopsyche*) were significantly more abundant in forested than pasture streams. Surprisingly, the filter feeder *Austrosimulium* was found in pasture streams and not forest streams. Ladle & Hansford (1981) reported that diatoms provide a better quality of food for blackflies than bacteria, and this may explain the greater abundance of *Austrosimulium* in pasture streams with abundant diatoms.

The general lack of response to shade of the common collector-browsers *Deleatidium, Zephlebia,* and the facultative shredder/browser *Olinga* in the channel experiments suggests that their densities are not controlled by local periphyton production. Other likely energy sources are particulate detritus from the catchment and upstream production, heterotrophic (bacterial and fungal) biofilms, and fine particulate carbon formed by precipitation. Rounick and Winterbourn (1983a) found that heterotrophic biofilms in a heavily shaded South Island beech forest stream were readily ingested and assimilated by *Deleatidium* and *Potamopyrgus*. A strong reliance on heterotrophic biofilms and/or detritus would explain the lack of shading effects on *Deleatidum* and *Zephlebia* in our channels. The landuse study indicated a markedly different shade response for the collector-browser mayfly *Deleatidium*, which was more abundant in forest streams than pasture streams. This indicates that factors other than shade and

primary production were important in determining response in the landuse comparison. Temperature did not vary significantly between channels, but in the open pasture streams daily maximum temperatures were typically 5–6ºC higher than in the shaded forested streams. For invertebrates with high upper thermal tolerances, such as the snail *Potamopyrgus*, the caddisfly *Pycnocentrodes*, and elmid beetle larvae (Quinn *et al.* 1994b), increased temperatures can greatly enhance biomass and production (Huryn *et al.* 1995). In contrast, these high temperatures may restrict the abundance of species with relatively low thermal tolerance, such as *Deleatidum* (Quinn *et al.* 1994b). Another possible factor is fine inorganic sediment, which is more abundant in pasture streams and which might adversely affect organisms.

The patterns of invertebrate preference for shade that we observed were very similar to those reported by Towns (1981) who used a black canopy to reduce the incident light by 94% in a small section (44 m^2) of the Waitakere Stream, near Auckland. Shading increased the densities of the filter-feeders *Austrosimulium* and *Aoteapsyche* and decreased densities of chironomids and *Pycnocentrodes*. Elmids and *Potamopyrgus* were not significantly affected. In Towns' experiment, shading also decreased the densities of the algal-piercing caddis *Oxyethira*, whereas this species showed no preference in our channels.

As well as generally confirming Towns' findings, our experiment indicates the *degree of shading* required to cause marked changes in the densities of shade-sensitive taxa. Over 60% shade was required to produce marked reductions in chironomid abundance and increases in *Austrosimulium*, whereas more than 90% shade was needed to produce significant reductions in taxonomic richness, reductions in *Pycnocentrodes* abundance, and increases in *Aoteapsyche* abundance.

Table 8 Summary of the effects of increasing shade on invertebrate abundance observed in the channel studies and landuse comparisons.

	Type	Functional group	Main expt.		Recol. expt.	Landuse comparisons
			Gravels	Tiles	Tiles	
Total biomass			Nd	nd	nd	
Taxa richness			(-)	-	(-)	
Total density			(-)	-		-
Chironomidae	Midge	G/CB	-	-	(-)	-
Deleatidium	Mayfly	CB			nd	+
Zephlebia	Mayfly	CB			nd	
Megaleptoperla	Stonefly	CB	-	nd	nd	nd
Helicopsyche	Case-caddis	G/CB	-	nd	nd	nd
Pycnocentrodes	Case-caddis	G/CB	(-)	-	(-)	nd
Olinga	Case-caddis	S/CB				nd
Oxyethira	Caddis	G(pi)	(-)			-
Aoteapsyche	Caddis	F	+	+	(+)	
Elmidae	Beetle	CG	(-)	note 1	note 1	
Latia	Limpet	G	(-)	(-)	(-)	nd
Potamopyrgus	Snail	G	(-)			-
Oligochaeta	Worm	CG	-	note 1	note 1	-
Austrosimulium	Sandfly	F	Note 2	+	(+)	-
Coloburiscus	Mayfly	F	Nd	nd	nd	(+)
Orthopsyche	Caddis	F	Nd	nd	nd	(+)
Zelandobius	Stonefly	CB	Nd	nd	nd	(+)

1. did not colonise the tiles
2. did not colonise the gravels

- denotes definite decrease
(-) denotes possible decrease

+ denotes definite increase
(+) denotes possible increase

nd denotes no data
blank denotes no change

G = grazer
CG = collector-gatherer

CB = collector-browser
F = filter-feeder
S = shedder
pi = algal piercer

NS = generalist feeder

3.5 Summary

1. Our streamside channel experiment mimics shading a short reach along a pasture stream, by changing light levels without changing water temperature, invertebrate drift or the supply of nutrients, dissolved or particulate carbon.

2. In the heavily shaded channels (90% and 98% shade) net photosynthesis was positive but low, and invertebrate grazing maintained a consistently low biomass. Thus, our first hypothesis, that shade reduces the growth rate and biomass of periphyton, was substantiated.

3. In the more open channels (0% and 60% shade) periphyton productivity was high but periphyton biomass was highly variable both in space and time. We infer that, for much of the time, loss processes (probably grazing) prevented biomass accumulations. Occasionally 'blooms' occurred in the unshaded channels, which indicates, however, that periphyton were released from 'top-down' grazer control (possibly by high water temperatures).

4. Our results suggest that to control periphyton in headwater streams it may not be necessary to reduce light levels to the very low levels typical of native forest streams (98% shade) but that shade of 60–90% may suffice.

5. Our second hypothesis, that shade would significantly affect periphyton community structure and function, was largely negated. Periphyton communities were dominated by diatoms under all four shade treatments, although filamentous and unicellular green algae were present in the open channels (0% shade). Shade had only a minor effect on photosynthetic pigment composition, although there was evidence that periphyton adapted to low light.

6. Our third hypothesis, that shade would affect nutrient uptake rate, was substantiated by a strong correlation between nitrate uptake rate and photosynthesis rate. Shaded streams act primarily as downstream 'transporters' of nitrate. By comparison, unshaded streams convert nitrate into periphyton biomass and store it in the channel during stable, low flows. In floods, the stored nitrogen is flushed downstream in particulate form.

7. Our fourth hypothesis, that shade would reduce total invertebrate numbers and taxonomic richness, was supported by both the channel study and landuse comparisons. The differences between pasture and forest stream, however, were smaller than might have been expected, because in shaded forest streams, high terrestrial carbon inputs (e.g., leaf litter) partly compensate for low periphyton productivity.

8. Several grazers (notably chironomids) and detritus feeding oligochaetes were less abundant in shaded channels as a result of decreased periphyton productivity.

9. Some grazers, collector-browsers, and collector-gatherers showed no shade response, presumably because they found ample food resources in both shaded and unshaded channels.

10. Two filter-feeders favoured high shade, presumably because they require attachment sites and clean water.

11. Invertebrates sensitive to high water temperature (e.g., *Deleatidium*) were unaffected by shade in our channel experiments (where shade did not affect temperature) but showed a preference for cooler forest streams in the landuse comparison.

4. EFFECTS OF STREAM AND RIPARIAN VARIABLES ON STREAM THERMAL RESPONSE

4.1 Introduction

Water temperature has a strong influence on stream ecosystem structure and function. Water temperatures outside the tolerance range of organisms excludes them from certain waterways, while temperatures outside their preferred range may adversely affect their metabolic rate and reproductive success. Consequently there is considerable interest in predicting changes in water temperature and the resulting ecological impact from activities such as abstraction and the removal or restoration of riparian vegetation. Riparian vegetation affects stream temperature in three main ways. Firstly, it absorbs a fraction of the incoming solar (shortwave) and atmospheric (longwave) radiation. This is most noticeable during cloudless summer days, when riparian shading reduces the daily maximum water temperature. Secondly, riparian vegetation emits longwave radiation, some of which reaches the stream. This is most noticeable on cloudless nights, when incoming riparian radiation partially offsets outgoing radiation emitted by the water, thereby increasing the daily minimum water temperature. Thirdly, riparian vegetation affects the stream microclimate (i.e., air temperature, humidity, and wind speed) which in turn affects the rates of evaporation, conduction, and longwave emission by the canopy and topography. Figure 29 shows the main radiation fluxes schematically. Because of the complexity of the problem, empirical studies have been unable to quantify precisely the effects of riparian shade on water temperature, but some success has been achieved using computer models. As has been described in Section 1, riparian vegetation, hillsides and stream banks all reduce the amount of solar radiation which reaches the stream water surface. In this section we quantify the effects of shade on stream water temperature using a combination of field measurements and a computer model (STREAMLINE) which we have developed and tested. The model predicts both the magnitude of temperature changes and the rates of heating or cooling in streams when riparian vegetation is either removed or restored. The model also suggests the likely effects of microclimate change on water temperature, although further work is required on how riparian vegetation affects wind speed, air temperature, and humidity near the stream channel.

Figure 29 Sketch showing the incoming and outgoing radiation fluxes for an idealised stream channel. Radiation is longwave (3–100 mm) except where marked 'shortwave' (<1400 nm).

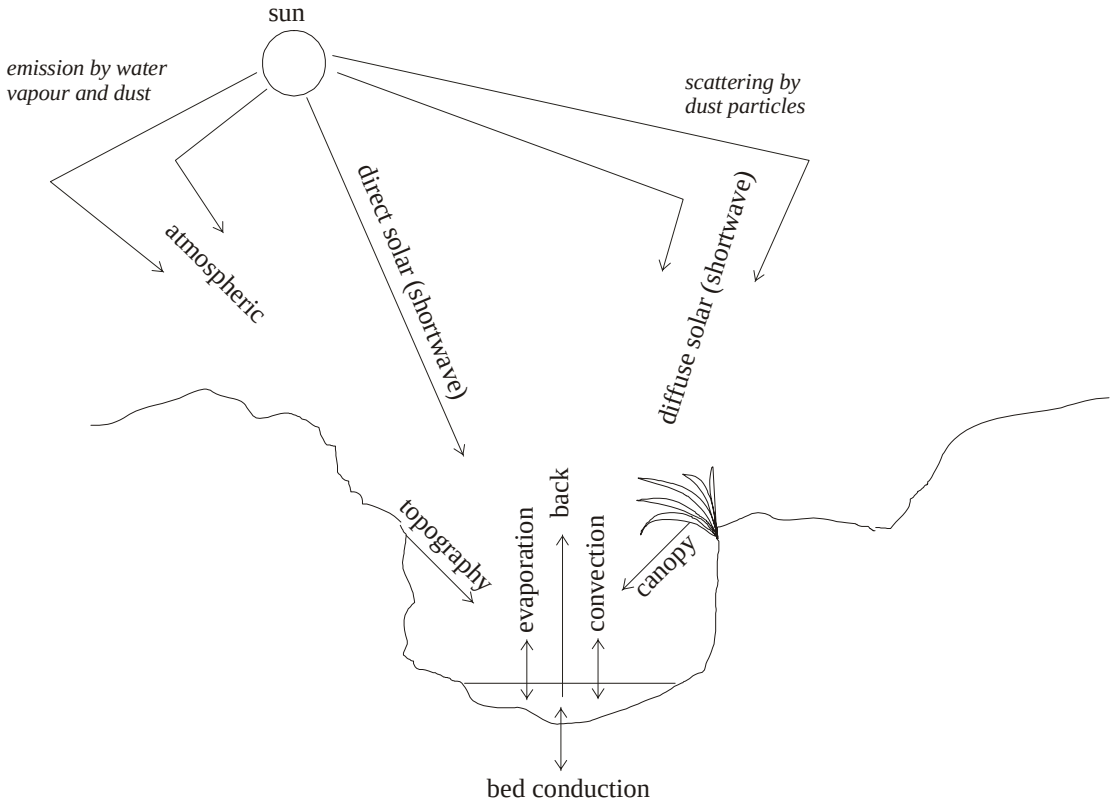

Previous New Zealand stream temperature studies

There are several well-documented examples in New Zealand of stream water temperature increases following the removal of riparian shade. Hopkins (1971) found that in summer, daily maximum water temperature in two small streams near Wellington which flowed from native bush into pasture increased by an average of 3–4ºC over a distance of 500 m up to 20.5ºC. The daily minimum temperatures remained much the same at 11–12ºC. Graynoth (1979) found that clearfelling to the stream edge of shallow streams in Nelson resulted in temperature increases in summer of up to 6.5ºC and decreases in winter of up to 2.5ºC. Water abstraction also has the potential to increase water temperatures because it decreases the mean water depth and, for a given surface heat flux, the rate of change of temperature is inversely proportional to the mean depth (Dymond 1983). Thus shallow streams have a smaller 'thermal inertia' than deep streams. Hockey *et al.* (1982) studied abstraction in the Hurunui River (low flow 20–50 $m^3 s^{-1}$) and found that summer daily maximum temperatures increased by approximately 0.1ºC for every 1 $m^3 s^{-1}$ drop in flow to a maximum of 25–26ºC at extreme low flows of about 10 $m^3 s^{-1}$. Dymond & Henderson (1981) studied the much smaller Stony River (summer flow 3 $m^3 s^{-1}$) and showed that an abstraction of 1 $m^3 s^{-1}$ increased maximum temperatures by 3ºC.

Several New Zealand native invertebrate and fish species favour cool water temperatures. Quinn & Hickey (1990) found that stonefly abundance declined markedly in New Zealand rivers once maximum summer temperatures exceeded 19ºC. In a laboratory study, Quinn *et al.* (1994b) found that the lethal temperature for invertebrates varied from 22.6–26.8ºC (*Deleatidium*, the most sensitive species tested) to 32.4ºC (*Potamopyrgus* and *Pycnocentrodes*, the two least sensitive species tested). Simons (1986) estimated that the upper temperature limit for the long-term survival of sensitive native species (smelt, banded kokopu, and inanga) was less than 26ºC. Richardson *et al.* (1994) found that smelt avoided the cooling-water plume below the Huntly power station once temperatures exceeded 26ºC and that inanga migration along the left bank past the station ceased once plume temperatures exceeded 27ºC. Hopkins (1971) found that several species of Trichoptera were less abundant at downstream pasture sites than at headwater native bush sites and suggested that this pattern may have been related to the temperature regime.

Stream temperature models

Computer models are used extensively to predict temperature in water bodies. For rivers these models fall into two groups: those concerned with predicting temperature rises below waste heat sources (e.g., below a power station cooling-water outfall) and those concerned with predicting changes in ambient temperature (e.g., resulting from flow abstraction, forest clearance, or revegetation). We do not discuss the first group of models. The second group uses the full heat balance equation to quantify each of the important heat fluxes across the water surface. There have been several modelling studies in large New Zealand rivers which use this approach: Jowett (1982) modelled the Whakapapa River; Hockey *et al.* (1982) modelled the effects of abstraction in the Hurunui River; and Dymond & Henderson (1981) used a heat balance model in the Stony River. In each of these studies riparian shading was ignored. Mason (1983) developed a computer programme for calculating the percentage shade of waterbodies of arbitrary shape and used it to estimate the daily radiation input to three small lakes in the North Island. He also applied the programme to a hypothetical rectangular river channel and showed that topographic shading could reduce radiation inputs by up to 45% and that the percentage shade calculated on the centreline of the channel was lower than the average shade over the channel width, typically by 10–20%. McBride *et al.* (1993) included the effects of shade in a heat budget model for the Mangatangi Stream, south-east of Auckland. They predicted that decreasing the minimum flow of the unshaded river from 1.0 to 0.2 $m^3 s^{-1}$ would increase the 5% exceedance temperature from 25.9 to 27.7ºC, but that replanting the banks with trees had the potential to reduce daily maximum temperatures. Several studies outside New Zealand have included the effects of shade in the heat balance equations: notably Brown (1969), Beschta & Weatheredd (1984) and Theurer *et al.* (1984). These studies were mainly concerned with predicting the temperature increases associated with forest clearance, although Theurer *et al.* (1985) predicted that replanting the banks of the

Tucannon River with trees had the potential to reduce maximum temperatures by 2ºC and to significantly improve the river's salmonid fishery. None of these models was entirely suitable for studying the effects of riparian shade in small streams and so we developed our own model (STREAMLINE). In this section we describe the model, discuss its testing using field measurements made in a small stream (PKL) at Whatawhata, and illustrate its use for predicting the effects of riparian management on stream thermal response.

4.2 The STREAMLINE model

The STREAMLINE model makes time-varying water temperature predictions in a non-uniform stream channel at steady flows. Model equations are summarised in Appendix 2. Only the main features of the model are summarised here. Flow is steady (does not vary with time) but non-uniform (varies spatially). The channel is divided into several segments and, in each segment, flow direction, discharge, velocity and depth are uniform. Tributary inflows can be specified at the top of any segment. In each segment, shade and bed sediment characteristics are also uniform. Parcels of water are released at fixed intervals of time and subsequently tracked along the channel, with results being stored whenever a parcel crosses a segment boundary. At each time step the heat fluxes into and out of each parcel are estimated using semi-empirical formulae (see Appendix 2) and the water temperature is updated. Model equations are solved using a fourth-order Runge Kutta scheme which is implemented in a FORTRAN programme. The model user enters data, runs the model and inspects results using a VISUAL BASIC interface programme which links dynamically to the main FORTRAN programme. Further details of the model are available on request.

Components of radiation

Water temperatures are affected by incoming and outgoing radiation across a wide range of wavelengths. As is commonly done in environmental studies (Monteith & Unsworth 1990) radiation is sub-divided into two components: shortwave radiation (300–1400 nm, the sum of: ultra-violet (300–400 nm), visible (400–700 nm) and near infra-red (NIR, 700–1400 nm)) and longwave radiation (3–100 mm). Shortwave radiation is emitted by the sun and reaches the stream either directly (termed 'direct' radiation) or after being scattered by particles in the atmosphere ('diffuse'). Longwave radiation is emitted by all bodies whose temperature is above absolute zero. Incoming longwave radiation reaches the stream from water, gas molecules and dust particles in the sky ('atmospheric'); from plant leaves, stems and trunks ('canopy'); and from hillsides and streambanks ('topographic'). Outgoing longwave radiation is emitted by the water ('back'). These radiation fluxes are shown schematically in Fig. 29.

The model assumes that all shortwave radiation is emitted, absorbed and scattered in the same 'average' way regardless of wavelength, and makes a similar assumption for

longwave radiation. This is clearly an oversimplification since absorption and scattering vary with wavelength, but is necessary in order to make the problem tractable. As discussed in Section 1, the plant canopy absorbs some components of solar radiation more strongly than others, and we discuss below the resulting difficulties.

Canopy and topography shade

Elevation angles are defined from the stream centreline to the top of the surrounding hills or streambanks (topography angles) and to the top of the trees, sedges, grasses etc. in the riparian zone (canopy angles) (Fig. 30). The model allows the user to specify topography and canopy angles in various azimuthal directions (relative to the direction of the channel) and it then interpolates linearly between these measurements. The topography and canopy angles are generally higher perpendicular to, than parallel with, the channel as shown by the hemispherical photographs in Spier & van Veen (1994) described in Section 1. The model allows the user to read in the time series of solar radiation measured at an unshaded site near the stream. It then assumes that, at times of clear sky, 80% of the solar radiation is direct and the other 20% diffuse (Monteith & Unsworth 1990). Alternatively, in the absence of measurements, the model estimates the incoming shortwave solar radiation using semi-empirical formulae (Tennessee Valley Authority 1972) which require information on latitude, Julian day number, elevation, dust content of the atmosphere, and cloud cover.

In order to calculate the amount of direct solar radiation which reaches the channel at each time step, the model calculates the solar azimuth (180° minus the angle of the shadow cast by the sun on a horizontal plane, measured from due north) and the solar elevation (the angle of the sun above the horizon) using standard formulae (Tennessee Valley Authority 1972).

These angles both vary with time: in summer the sun rises to the south of east, tracks north and climbs higher in the sky during the morning until at solar noon it is due north and at its zenith. During the afternoon the sun sinks and tracks west, setting to the south of west. At each time step the model calculates the topography and canopy angles looking in the direction of the sun. When the solar elevation angle is less than the topography angle, no direct solar radiation reaches the channel. When the solar elevation lies between the topography and canopy angles, a fixed percentage (defined by the ‘shade factor’) of the incoming radiation (both shortwave solar and longwave atmospheric) is absorbed by the canopy (see Fig. 30).

Figure 30 Sketch of a typical channel cross-section in PKL stream showing topography and canopy angles perpendicular to the stream. Note: topography and canopy angles vary with azimuthal angle (see text for details).

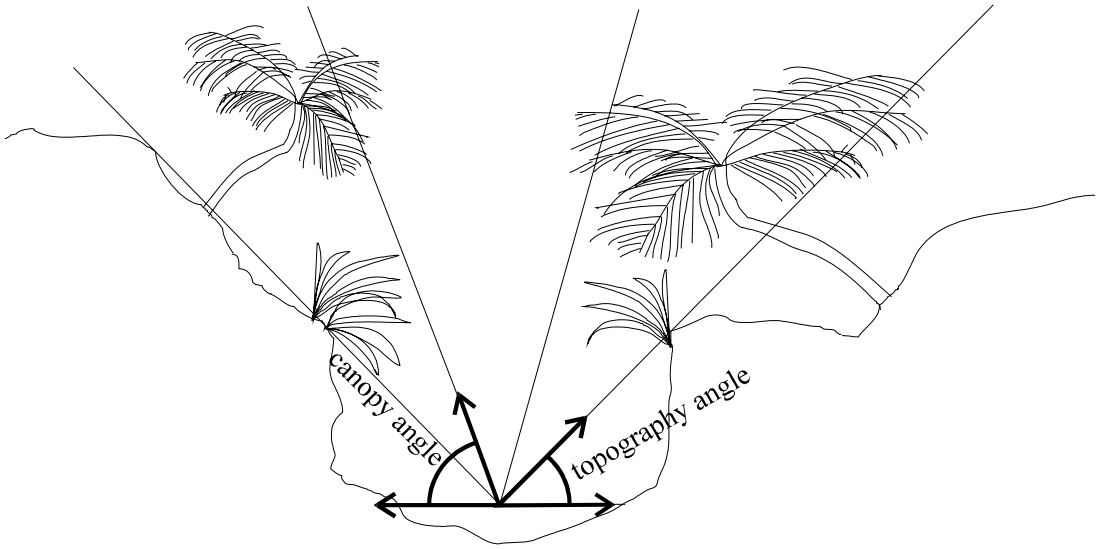

The model assumes that diffuse solar (shortwave) and atmospheric (longwave) radiation are emitted uniformly by all parts of the sky. This is only approximate since the luminance of the sky can be up to three times higher in the corona around the sun than elsewhere. For each stream channel segment a single integration is made at the beginning of each model run to calculate the fraction of the total available diffuse radiation which reaches the channel (Mason 1983).

Bed conduction

In shallow streams the transfer of heat into and out of the streambed affects water temperatures (Comer & Grenney 1977). As a first approximation, we modelled heat transfer as conduction (Jobson 1977). By setting the conduction coefficient to zero, streambed conduction can be neglected.

Figure 31 Sketch showing the net fluxes in the arcs of the canopy and topography for two alternative sub-models of longwave radiation. α_1 and α_2 = topography and canopy angles; E_w, E_c and E_t = longwave radiation fluxes emitted by the water, canopy and topography respectively.

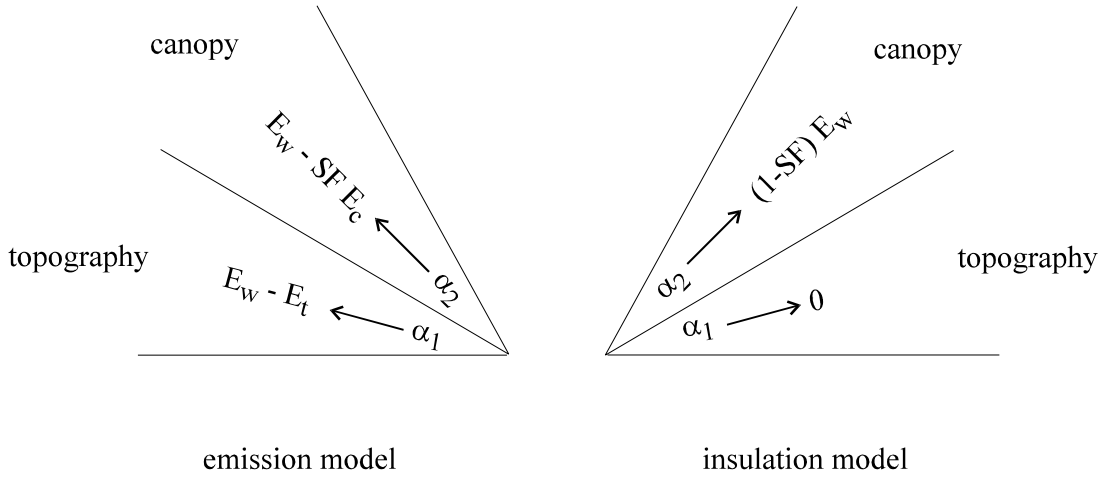

Canopy and topography radiation

Riparian vegetation, hillsides, stream banks and the water itself all emit longwave radiation (see Fig. 29). The model user can choose between two alternative sub-models for longwave radiation. In the first, the temperature and emissivity of the canopy and topography are defined by the user and the emitted radiation is calculated using the Stefan-Boltzmann equation (see equation A13). Radiation is only emitted from that proportion of the canopy which is defined by the 'shade factor'. This sub-model requires *a priori* information about canopy and topography temperatures, and these are frequently approximated by measured air temperatures (Beschta & Weatheredd 1984). In the study described below we assumed standard values for the emissivity of the canopy (0.95) and the topography (0.90) (Tennessee Valley Authority 1972). This can be termed the 'emission' sub-model. One potential difficulty with this approach is that air temperature is commonly only measured at a climate station located some distance away from the stream channel (e.g., an airport) and may not accurately quantify canopy and soil temperatures in the channel. The model user can choose an alternative sub-model (termed the 'insulation' sub-model) in which it is assumed that a fixed percentage (we assumed 100%) of the longwave radiation emitted by the water in the direction of the topography and canopy is absorbed and re-emitted. This is equivalent to assuming that there is no net outgoing longwave radiation through either the topography or that fraction of the canopy defined by the 'shade factor'. The 'emission' and 'insulation' sub-models are compared schematically in Fig. 31.

4.3 Field study

Site description

Two heat budget experiments (December 1993, April 1995) were conducted in a small second-order stream (PKL, Pasture Kiripaka Leftbank tributary) at Whatawhata, near Hamilton. PKL rises in native bush and flows some 600 m through pasture before joining the larger Kiripaka Stream (see Fig. 32). It is second-order where it leaves the bush and becomes third-order where it is joined by the tributary. PKL has a mean flow of 5–10 L s^{-1}, a mean channel width of just over 1 m, and a mean depth of about 10 cm. For most of its length PKL is incised about 1 m between banks typically 2 m apart at banktop height, with overhanging bankside vegetation comprising grasses, sedges and ferns. There are occasional tree ferns and mahoe trees on the streambanks, but shading is principally by the surrounding hillsides, the stream banks and the overhanging bankside vegetation. The streambed comprised gravels and sands with occasional boulders overlying an impermeable layer of grey clay.

Figure 32 Sketch map of PKL stream. For modelling purposes the stream is sub-divided into four homogeneous sub-reaches: 'top' (0–165 m), 'open' (165–220 m), 'canyon' (220–490 m) and 'bottom' (490–560 m).

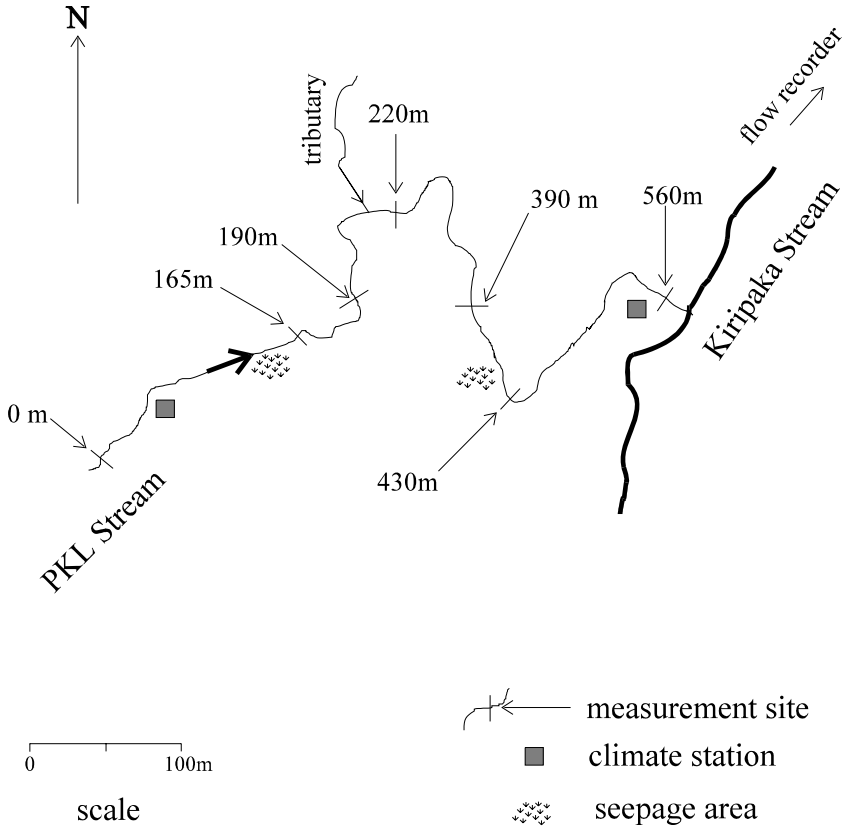

Methods

PKL stream was surveyed to determine: channel geometry (azimuth and width at water level), shade geometry (width at banktop height, bank height, percentage shade by visual assessment, angle of elevation of the hills in each of four azimuthal arcs, and the thickness of the gravel layer). Based on survey results, four reaches were identified: 'top' (0–160 m), 'open' (165–220 m), 'canyon' (220–430 m) and 'bottom' (430–650 m) (Table 9). Flows were gauged several times, velocities measured using dye tracer, and reach-averaged depths calculated from $h = q / ub$ where q = flow from gaugings (which varies from reach to reach and with time); b = average width from surveys (assumed uniform and independent of flow); and u = mean velocity from dye tracing and gaugings. Thermistors recorded water temperature at six points along the channel (0, 165, 190, 220, 430 and 560 m, see Fig. 32), in the tributary and at a depth of 10 cm in the sediment at two points (190 and 390 m). Seepage temperatures were surveyed once and seepage flows estimated from gauged stream flows by difference. Two climate stations adjacent to the stream channel measured solar radiation, air temperature, wind speed and direction, and atmospheric pressure at 15 minute intervals. Cloud cover and humidity were measured at Auckland (90 km away) and Hamilton (30 km) airports. Total incoming and outgoing radiation (shortwave plus longwave) was measured just above the water surface in a shaded part of the channel (390 m).

Results

Two periods of steady flow were identified: 12–16 December 1993 (calibration) and 5–7 April 1995 (testing). Table 9 summarises data for each period. Flow increased along the channel (Fig. 33) because of the tributary at 230 m and other seepage inflows. We measured the average seepage temperature to be 15ºC in December 1993 and 16.5ºC in April 1995. The channel width averaged 1.17 m (range 1.02–1.35 m) and did not change significantly with flow. Mean velocities measured during gaugings and using dye averaged 0.075 m s^{-1} (range 0.049–0.132 m s^{-1}) and 0.064 m s^{-1} (range 0.049–0.078 m s^{-1}) respectively. At the low flows studied (5–10 l s^{-1}) high variability disguised any relationship between velocity and flow and so we assumed a constant velocity of 0.070 m s^{-1}.

For each segment we estimated the flow using Fig. 33, assumed constant velocity and width, and calculated the mean depth as described above. The elevation angle of the hillsides measured from banktop averaged 30º (top and canyon reaches), 25º (bottom) and 15–25º (open). We set the topography angle looking up stream and down stream equal to the angle of the hillsides. From the water surface the hills are often hidden by the banks when looking perpendicular to the stream. From field measurements the topography angles perpendicular to the stream channel varied 40–55º (top reach), 15–25º (open), from 55–60º (canyon) to 25º (bottom).

Table 9 Summary of channel and topography data

Segment	Reach	distance (m)	azimuth (deg.)	topography (parallel) (deg.)	topography (perpend.) (deg.)	canopy (deg.)	temp. (ºC)
Pegs AB	Top	30	35	30	50	90	logger
Pegs CD	Top	53	71	30	55	90	
Fenceflap	Top	115	71	30	40	90	logger
Pegs HI	Top	165	58	30	55	90	
White box	Open	190	353	25	25	90	logger
Pegs M	Open	220	353	15	15	90	
Pegs LNOP	Canyon	300	65	30	55	90	
Blackberry	Canyon	430	170	30	60	90	logger
VWYXZ	Bottom	540	50	25	25	90	
ZZ+	Bottom	560	123	25	25	90	logger

Width, 1.17 m; bed layers, 10; bed thickness, 0.05 m; bed heat capacity, 2167 kJ K^{-1} m^{-3}; bed heat conduction coefficient, 50 kJ K m^{-1} hr^{-1}

Figure 33 Gauged flows in PKL stream (circle) and its tributary (triangle) expressed as a percentage of the flow in the Kiripaka Stream. The solid line is the distribution assumed in the modelling.

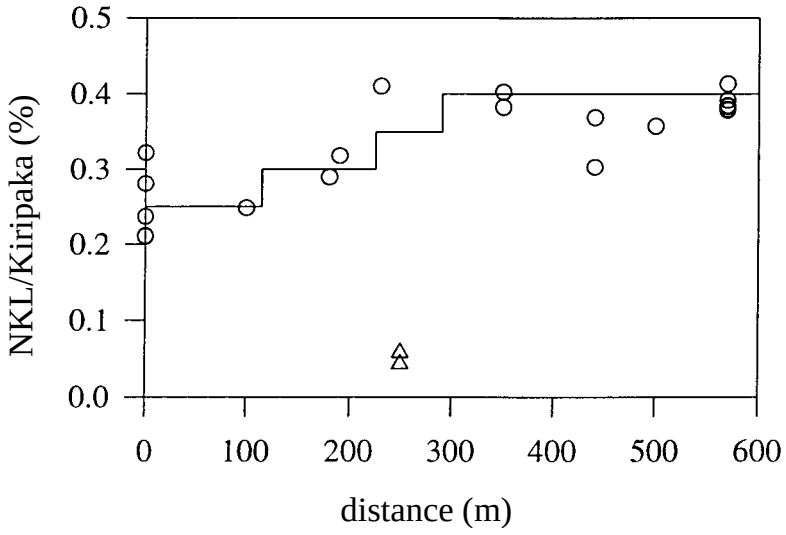

4.4 Model calibration

During the calibration period (12–16 December 1993) riparian vegetation (grasses, sedges, and ferns) or aquatic macrophytes (predominantly water cress) extended across the entire channel in most parts of the stream, although there were numerous gaps in the canopy. Accordingly we assumed a canopy angle of 90° in all segments (i.e., complete canopy closure) and a shade factor less than unity (i.e., gaps in the canopy). The bed was modelled as 10 layers 0.05 m thick, the underlying clay layer was assumed non-conducting, and we adopted literature values for sediment specific heat capacity (2170 kJ m^{-3} K^{-1}) and thermal conductivity (50 kJ hr^{-1} m^{-1} K^{-1}) (Jobson 1977). Model coefficients are summarised in Table 10.

The predicted daily maximum temperature is strongly influenced by shade factor but is fairly insensitive to variations in meteorology (wind speed, humidity, air temperature etc.) and bed conduction parameters (details omitted). The reason is that the daily maximum temperature depends largely on the amount of shortwave solar radiation which reaches the water during daylight hours, and this in turn depends on the topography angle, canopy angle and shade factor. We calibrated the model by varying the shade factor until a satisfactory match was obtained between predicted and observed maximum daily temperatures. Figure 34 shows that a remarkably good calibration was achieved using shade factors of 0.30 (top and canyon reaches), 0.10 (open) and 0.20 (bottom reach).

Predictions made assuming that the canopy and topography are emitters were barely distinguishable from predictions made assuming they are insulators (Fig. 35). This was in spite of the fact that the radiation fluxes involved were quite large: the emission model predicted longwave radiation fluxes of 1350 (water), 100–200 (canopy), 200–600 (topography), and 400–900 kJ m^{-2} hr^{-1} (atmosphere). For the emission model, we found that the predicted outgoing flux from the water emitted into the arcs of the topography and canopy angles almost exactly matched the incoming flux emitted by the topography and canopy. Thus the net longwave radiation flux in the arcs of the topography and canopy angles was negligibly small, matching the assumption made in the insulation model.

Table 10 Summary of parameters used during model calibration

CALIBRATION December 1993								
Segment	distance (m)	Velocity (m s^{-1})	depth (m)	Inflow (L s^{-1})		temp. (ºC)	Flow (L s^{-1})	shade factor
pegs AB	30	0.07	0.0855	7		Logged	7	0.3
pegs CD	53	0.07	0.0855	0			7	0.3
fenceflap	115	0.07	0.0855	0			7	0.3
pegs HI	165	0.07	0.1025	1.4	seepage	15	8.4	0.3
white box	190	0.07	0.1025	0			8.4	0.1
pegs M	220	0.07	0.12	1.4	tributary	logged	9.8	0.1
pegs LNOP	300	0.07	0.137	1.4	seepage	15	11.2	0.3
blackberry	430	0.07	0.137	0			11.2	0.3
VWYXZ	540	0.07	0.137	0			11.2	0.2
ZZ+	560	0.07	0.137	0			11.2	0.2

Figure 34 Model calibration: observed and predicted water temperatures at three sites on PKL stream, 12-16 December 1993.

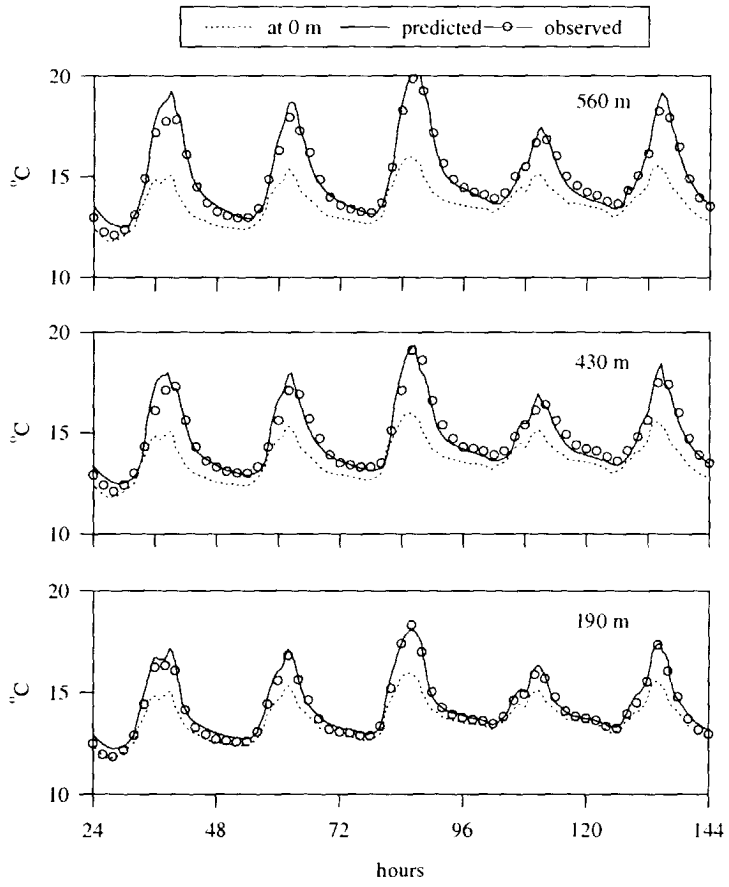

Table 11 Summary of parameters used during model testing

	TESTING April 1995							
Segment	**distance (m)**	**velocity ($m\ s^{-1}$)**	**depth (m)**	***inflow*** **($L\ s^{-1}$)**		**temp. (ºC)**	**flow ($L\ s^{-1}$)**	**Shade Factor**
pegs AB	30	0.07	0.0977	8		logged	8	0.1
pegs CD	53	0.07	0.0977	0			8	0.1
Fence flap	115	0.07	0.0977	0			8	0.1
pegs HI	165	0.07	0.1172	1.6	seepage	16.5	9.6	0.1
White box	190	0.07	0.1172	0			9.6	0
pegs M	220	0.07	0.1368	1.6	tributary	logged	11.2	0
pegs LNOP	300	0.07	0.1563	1.6	seepage	16.5	12.8	0.15
Blackberry	430	0.07	0.1563	0			12.8	0.15
VWXYZ	540	0.07	0.1563	0			12.8	0.05
ZZ+	560	0.07	0.1563	0			12.8	0.05

Figure 35 Comparison of water temperatures at 560 m predicted assuming that the canopy and topography are `reflectors' (solid) and `emitters' (dashed) of longwave radiation.

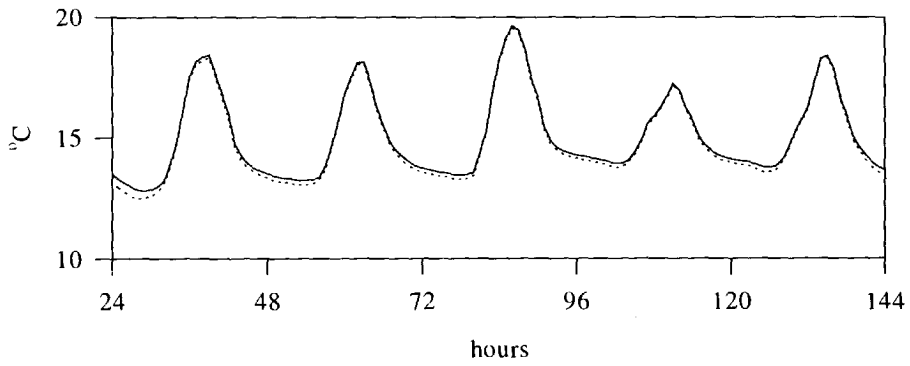

4.5 Model testing

Just prior to the testing period (5-6 April 1995) there was a flash flood which removed a substantial amount of grass, sedge and fern from the stream banks and all the watercress from the channel. Based on visual assessments we reduced the shade factor to 0.10 (top reach), 0.15 (canyon), 0.05 (bottom) and 0.00 (open) while retaining our previous assumption of complete canopy closure (canopy angle 90°) (see Table 11). Other coefficients remained the same. Figure 36 shows that the magnitude of the observed and predicted daily maximum and minimum temperatures matched reasonably well, although the model predicted daily maximum temperature slightly earlier than was observed. We suspect that this arises because of slight measurement errors in topography angle. In April the solar elevation was markedly lower than in

December and the sun was more frequently obscured by the stream banks and hillsides.

Figure 36 compares observed and predicted streambed temperatures (at a depth of 10 cm). The observed diurnal variation (3ºC) was only slightly smaller than that observed in the overlying water (4ºC), indicating that there was either rapid conduction of heat or, more likely, substantial advective exchange of interstitial water between the bed and the overlying water. The observed daily maximum and minimum temperatures matched fairly well at 560 m (although the same timing error occurred in streambed and water temperatures) while at 190 m the model underestimated streambed temperature slightly. Given the simplified nature of the streambed conduction model, the observed and predicted temperatures matched reasonably well.

Figure 37 compares longwave radiation fluxes predicted by the model at 390 m with the total radiation flux (longwave plus shortwave) measured 10 cm above the water surface at mid-channel. We did not deploy upward or downward facing shortwave sensors in the stream channel and so cannot separate the measured total flux into shortwave and longwave components. Consequently during daylight (hours 132–135) there were significant differences: the measured outgoing radiation was slightly higher than the predicted longwave radiation emitted by the water because of reflected shortwave solar radiation, while the measured incoming radiation was higher than the predicted incoming longwave radiation because of direct and diffuse shortwave solar radiation. At night (hours 135–143) when the shortwave radiation flux was negligible, there was a close correspondence between: the measured outgoing radiation and the predicted back radiation flux emitted by the water; and the measured incoming radiation and the sum of the predicted longwave radiation fluxes reaching the water surface from the atmosphere, canopy and topography.

Figure 36 Model testing: predicted (solid) and observed (o) water and streambed temperatures at 10 cm on 5-6 April 1995 at 190 m and 560 m. Water temperatures at 0 m are shown dashed.

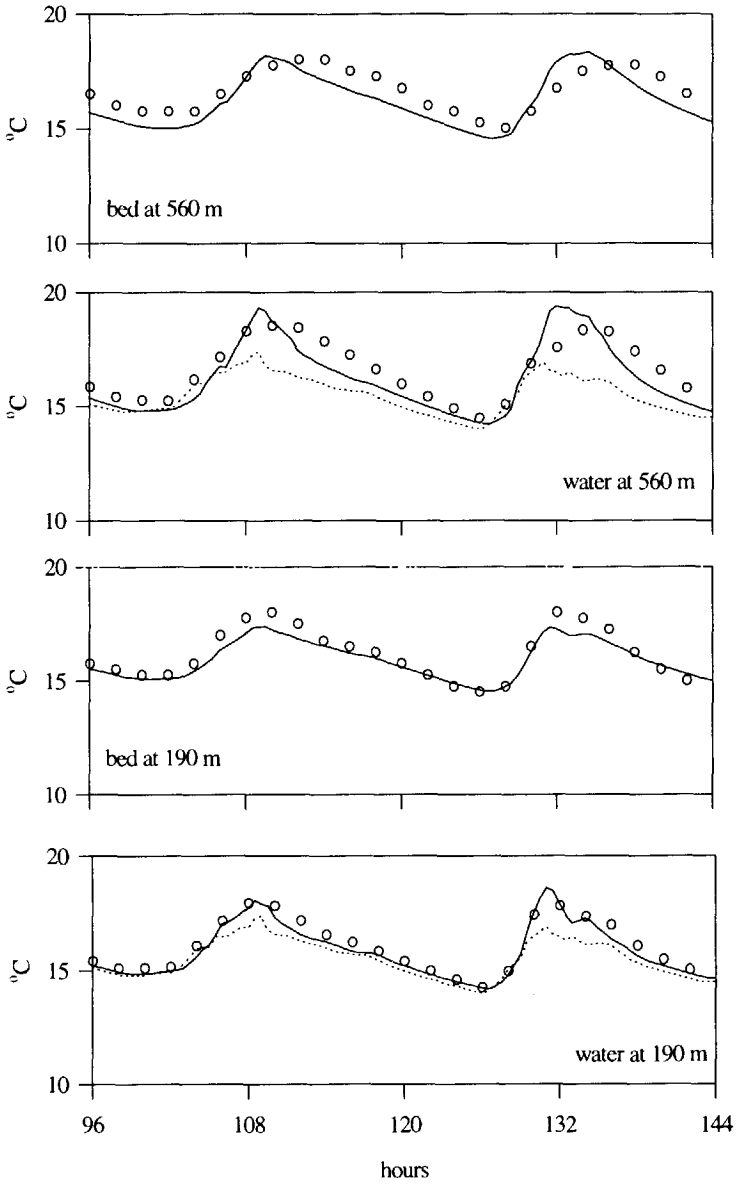

Figure 37 Comparison of observed (symbols) and predicted (lines) incoming and outgoing longwave radiation at 390 m. Note the predicted incoming radiation is the sum of atmospheric, canopy and topography radiation.

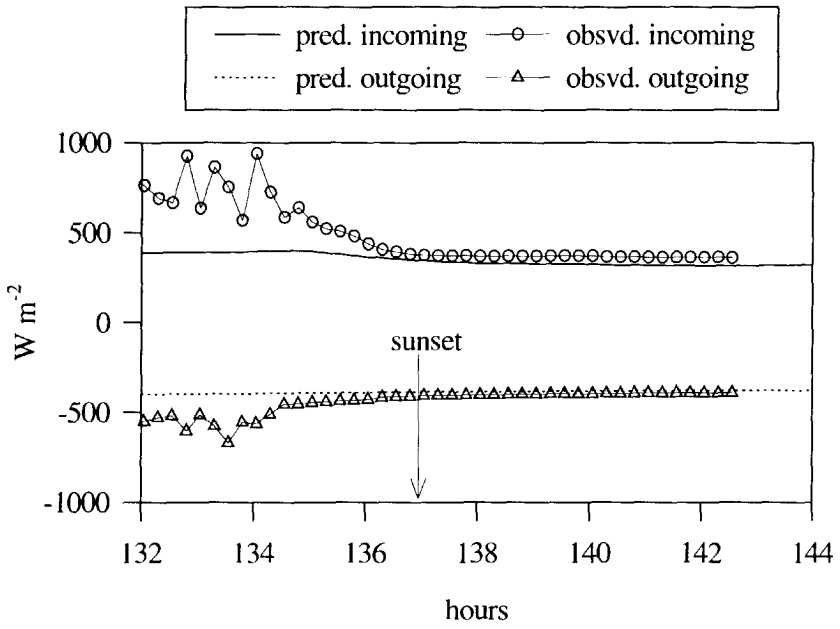

4.6 Accuracy of the model

Model assumptions

The STREAMLINE model makes three simplifying assumptions when quantifying shade. Firstly, it assumes a constant ratio of diffuse to total solar radiation (20%). This figure is appropriate on bright, sunny days, but as the cloud cover increases this ratio decreases until on heavy, overcast days it approaches 100%. We are principally concerned with extreme temperatures and, consequently, during model calibration and testing we focused our attention to predicting temperatures on sunny days.

Secondly, the model assumes that a constant fraction of the incoming radiation is absorbed by the canopy regardless of solar elevation. Typically the fraction of incoming radiation transmitted by the canopy increases as solar elevation increases and, hence, the path length through the foliage decreases. In PKL much of the canopy shading is from overhanging grasses, sedges, logs and ferns (Fig. 30) so that our assumption of constant shade factor may be realistic. The fact that the model successfully predicted the observed diurnal pattern of water temperature indicates that any errors are either small or are attenuated by the thermal inertia of the water and streambed. Beschta & Weatheredd (1984) developed a model which calculates the pathlength of radiation through the canopy as a function of time, knowing the geometry of the riparian forest and assuming a constant light attenuation coefficient. Were the model to be applied to situations where shading is primarily by riparian

forest, then consideration should be given to modifying the way the STREAMLINE model handles canopy shade, with the proviso that field survey methods should not become unduly onerous.

Thirdly, the shading model assumes that once the solar elevation exceeds the topography angle, the entire channel receives direct solar radiation (albeit after some absorption by the canopy). Conversely when the solar elevation is less than the topography angle, the channel receives no direct solar radiation (although it does receive diffuse solar and atmospheric radiation). Since the topography angle is measured from the stream centreline, in effect the model predicts the direct solar radiation flux at *mid-channel* and applies this flux uniformly across the whole stream. Strictly this assumption is valid only if the channel azimuth equals the solar azimuth throughout the day. In practice, however, the solar azimuth varies throughout the day and the banks shade a portion of the channel: the portion varies depending on the solar and stream azimuth, solar elevation, and bank height. The same logic applies to the way the model calculates the total diffuse solar radiation and atmospheric radiation fluxes. It is possible to model the changes with time of the portion of the channel which is shaded from direct and/or diffuse radiation by the banks (Mason 1983, Theurer *et al.* 1984), given survey information describing the geometry of the banks and riparian vegetation. In PKL, however, the bank heights, channel widths and channel azimuth are highly variable and we chose to use a more economical shade model. Mason (1983) showed that the daily total radiation flux at mid-channel is higher than the average flux over the whole stream channel by as much as 10–20%. Our model of PKL successfully predicts stream temperatures. If our simplified model of topographic shade overestimates the incoming radiation flux by 10–20% (as suggested by Mason 1983) then there must be a compensating error elsewhere: most likely the canopy shade factor is overestimated by 10–20%.

Net radiation balance

During model calibration and testing, a satisfactory match was achieved between observed and predicted water temperatures, which indicates that the *net* heat fluxes were predicted with tolerable accuracy both during the day (when solar radiation fluxes are high) and at night (when only longwave radiation fluxes are significant). This is no guarantee that each of the individual fluxes is predicted correctly by the model (i.e., there could be compensating errors in two or more fluxes). The fact that the amplitude of diurnal temperature variations was predicted correctly, however, indicates that the shortwave fluxes are predicted reasonably well and, if there are compensating errors, they are most likely to be present in the longwave radiation balance.

Longwave radiation balance

The fluxes of incoming (atmospheric, canopy and topography) and outgoing longwave radiation (back radiation) are both large and vary little with time. Their net effect, however, strongly affects the predicted temperature. We measured incoming atmospheric radiation for 48 hours at an unshaded site in Hamilton using total and shortwave radiation sensors (the difference gives the incoming longwave atmospheric radiation). We also measured cloud cover and air temperature and calculated the atmospheric radiation using Swinbank's formula corrected for cloud (Tennessee Valley Authority 1972) which is used in the STREAMLINE model. Figure 38 shows that there was very close agreement between the observed and predicted fluxes (RMS error < 5%), which gives us confidence that the model predicts accurately the total available atmospheric radiation flux prior to shading by topography and canopy.

Figure 38 Comparison of hourly averaged measured incoming longwave radiation (circles) with incoming atmospheric radiation predicted using Swinbank's formula (line).

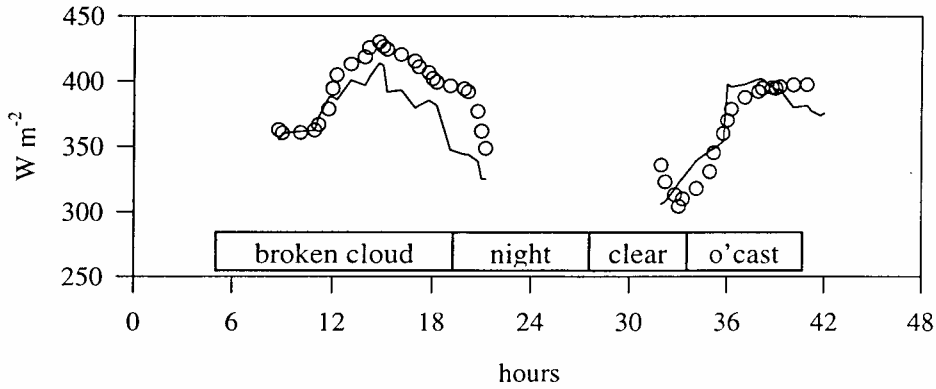

Figure 37 shows that there was close agreement at night between observed and predicted incoming and outgoing total longwave radiation. There is no guarantee, however, that we correctly apportioned the total flux between its separate components (viz., canopy, topography and atmospheric radiation). We were unable to measure these components separately. These fluxes are all predicted from the Stefan-Boltzmann formula (see Appendix, equation A13) and at PKL we assumed the same temperature for all three emitters (the measured air temperature) together with very similar emissivity values (0.90–0.95). Consequently it is possible to make large changes in the topography angle, canopy angle and/or shade factor within the model without significantly changing the predicted incoming longwave radiation flux. Thus we cannot state with confidence that at PKL the model successfully predicted the individual incoming (canopy, topography, and atmospheric) and outgoing (water) longwave radiation fluxes, but apparently the model correctly predicted the net flux.

Shortwave radiation fluxes

Correct prediction of the solar radiation flux requires correct estimation of the topography angle, canopy angle, and shade factor. At PKL the topography and canopy angles were measured (to within a few degrees) and the shade factor was adjusted until observed and predicted water temperatures matched. To check our calibrated shade factors we compared observed and predicted diffuse non-interception (DIFN) values. DIFN measures the ratio of diffuse radiation flux at the water surface to incident flux (see Section 1 for a more detailed description). Spier & van Veen (1994) surveyed PKL stream in February-March 1994 using a canopy analyser (see Section 1) and made 27 DIFN measurements at sites 20 m apart along the length of the stream at transverse locations alternating between 10, 30, 50, 70 and 90% of channel width. The measured DIFN varied from 0.38 (canyon) to 0.88 (open reach) (Table 12). A further 27 measurements made along the channel centreline gave very similar mean values (details omitted). DIFN values vary both along and across the channel which gives rise to large standard deviations in the average measured DIFN values (Table 12). Model results include incident diffuse radiation and the diffuse radiation flux which reaches the water surface after topographic and canopy shading. The ratio can be termed the 'model DIFN' and is directly comparable with the measured DIFN. Note that in PKL, measured DIFN values are not low enough to be biased by the fact that plants absorb visible light more efficiently than NIR (see Section 1, Fig. 5).

Table 12 Comparison of observed and predicted diffuse non-interception (DIFN) values in PKL stream. The model DIFN varies because topography and canopy angles vary slightly within a reach.

reach	distance	measured DIFN mean ± standard deviation (number)	Model DIFN calibration, Dec. 1993
top	0–165	0.47 ± 0.29 (7)	0.41 ± 0.02
open	165–220	0.88 ± 0.37 (5)	0.79 ± 0.02
canyon	220–430	0.38 ± 0.29 (9)	0.36 ± 0.02
bottom	430–560	0.72 ± 0.39 (6)	0.66 ± 0.02

None of the model DIFN values is significantly different from the measured DIFN values at the 95% confidence level. It should be noted that differences would need to be quite large in order to be statistically significant because of the large standard deviations in the measured DIFN. We can conclude that at PKL there is fairly good agreement between model predictions of total shade (topography plus canopy) and field measurements made using the canopy analyser. Although we can separate the effects of topographic and canopy shading in the model, there is no way of reinterpreting Spier & van Veen's field results in this way because the canopy

analyser does not distinguish between topographic and canopy shading. This means that at PKL we cannot compare model shade factors with direct field measurements of the shade factor. In future calibration and testing studies we may be able to shield the canopy analyser sensor so that it only looks through the canopy in which case we will measure the DIFN value of the canopy (i.e., measure directly the canopy shade factor).

Emission and insulation sub-models

It is somewhat fortuitous that the emission and insulation sub-models for longwave canopy and topography radiation give almost identical results, because in the model there is no direct coupling between water temperatures and canopy or topography temperatures. In nature such coupling does exist: canopy and topography temperatures are affected by variations in solar and atmospheric radiation in the same way as water temperature. For example, solar radiation striking the stream banks increases the soil temperature thereby increasing the longwave radiation flux emitted by the topography. This process is expected to be particularly important in narrow, incised streams such as PKL. The emission model requires the user to specify topography and canopy temperatures *a priori*. During our experiments we did not measure these temperatures directly but simply assumed they could be approximated by air temperature measured some tens of metres away from the channel. We can infer from our results that this assumption is realistic. Commonly in stream temperature prediction studies the only available meteorological data are from climate stations far distant from the channel (e.g., from airports). In this situation it may not be satisfactory to approximate canopy and topography temperatures using measured air temperatures. Our results indicate, however, that the insulation model, which does not require temperatures to be specified, is capable of predicting the net longwave radiation balance quite satisfactorily. Consequently if there is reason to believe that the available air temperature data are not representative of the microclimate close to the stream channel, then our suggested insulation model should prove to be superior to the standard emission model.

Thermal response of PKL stream

From Fig. 34 it can be seen that daily maximum water temperatures in PKL, initially low where the stream leaves the native bush, increase on sunny days by 5–6ºC over a distance of 600 m. This is in accord with the rise of 3–4ºC over 500 m observed by Hopkins (1971) in a small stream near Wellington and an increase in summer of up to 6.5ºC observed by Graynoth (1979) for an open stream in Nelson. The daily maximum temperature depends largely on the shortwave solar radiation flux which reaches the water during daylight hours. This means that in a pasture stream such as PKL (where the canopy shade factor is fairly small but the topography angles are large) the accurate prediction of water temperature requires the accurate assessment of topography angles. Figure 34 also shows that, whereas the daily maximum increased

increased by 5-6°C, the daily minimum only increased by 1.0-1.5°C. The daily minimum temperature, occurring near dawn, depends on the longwave radiation balance between incoming radiation from the atmosphere, canopy and topography and outgoing radiation from the water. The longwave radiation balance is strongly influenced by the air temperature, which determines the longwave radiation emission from the atmosphere, canopy and topography. The streambed also plays a role. The bed warms up during the day as heat is conducted from the water into the sediments but when water temperatures fall at night, heat is conducted from the bed to the water thereby reducing the rate of heat loss from the stream. Figure 39 shows the predicted water temperatures in PKL stream 500 m from the edge of the bush for three different shade factors (0.00, 0.30 and 0.95). For these simulations the stream is assumed to be uniform with an average topography angle of 45° and seepages are ignored. It seems likely that, were the original native bush cover still present, the maximum daily stream temperature would be of the order 15°C whereas with its present riparian vegetation (i.e., grasses, sedges, ferns and logs) it is typically 20°C. Were the present riparian vegetation to be removed (e.g., by heavy stock grazing or spraying), then the stream would only be shaded by the banks and surrounding hills, in which case maximum temperatures could be expected to rise to about 22.5°C.

Figure 39 Predicted temperatures 500 m from the bush edge in PKL stream for three different shade factors.

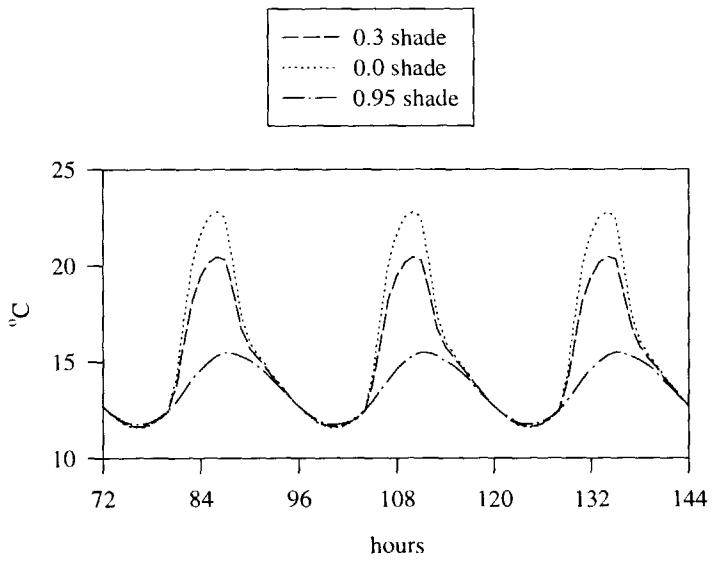

4.7 Model predictions

Equilibrium temperature

The equilibrium temperature is the temperature predicted in a very long uniform channel with no inflows. The STREAMLINE model was used to predict the equilibrium temperature and the rate of heating of a second-order stream (similar in size to PKL) flowing from a heavily shaded reach (e.g., native bush) into an unshaded (e.g., pasture) reach. The stream was assumed uniform and to flow north-south with a topography angle of 45° which was independent of azimuth angle. The canopy angle was 90° (i.e., canopy closure) and the shade factor 0.30 (the average calibration value). We fitted smooth sine curves to the measured air temperature (daily range 10–20°C) while humidity (90%) and wind speed (1 m s^{-1}) were assumed constant at the average measured values. Seepage inflows were neglected. We assumed that the water temperature at the edge of the native bush was equal to the equilibrium water temperature predicted by the model in the same channel with the same humidity and wind speed but with a shade factor of 0.95. This predicted temperature pattern closely approximated the water temperatures measured at the top of PKL stream. Figure 40 shows predicted water temperatures at various distances down stream from the point where the stream flow first enters the pasture. The daily maximum temperature increases with distance down stream and at a distance of 500 m below the edge of the bush (roughly equivalent to the last sampling point on PKL) has risen by 6–7°C (which is comparable with the increase measured in PKL). An important feature of Fig. 40 is that with increasing distance down stream, the difference between temperature profiles at adjacent sites decreases, so that the profiles at 5 and 10 km are barely distinguishable. This particular second-order stream takes about 5 km to adjust from its thermal regime under dense native bush and reach a new dynamic equilibrium. Maps of the study area show that first-, second-, and third-order streams are typically 1, 2, and 5 km long.

Temperature changes and rates of change

Two questions arise when considering riparian shade and stream water temperature: what temperature decrease/increase is likely to occur as a result of planting/removing riparian shading, and over what length of channel do these temperature changes occur? Figures 41 and 42 summarise daily maximum water temperatures predicted in streams of increasing size (i.e., mean depth) with different levels of shade. These predictions are discussed in more detail in Collier *et al.* (1995), where results are also presented for the daily minimum water temperature. The hydraulic parameters of the streams used in these predictions are summarised in Table 13. Shade is expressed in terms of daily total radiation. Solar radiation, air temperature, wind speed, relative humidity and barometric pressure were set to the long-term average values measured at Whatawhata (New Zealand Meteorological Service 1986). The initial temperatures

were the predicted equilibrium temperatures for 95% shade. Air temperature, humidity and wind speed were assumed identical in the bush and pasture reaches, and only the percentage shade was altered. Based on measurements at Whatawhata, the 25% shade factor represents a low bound of shade, 50% is more typical of small pasture streams, and 75% is typical of small streams with sparse tree plantings along the banks.

Table 13 Summary of channel parameters used in Figs 41 and 42.

	First-order	Third-order	Fifth-order
flow ($m^3 s^{-1}$)	0.013	0.080	0.250
width (m)	1.3	1.6	3.3
mean depth (m)	0.10	0.30	0.50
mean velocity ($m s^{-1}$)	0.10	0.165	0.15

Figure 40 Temperature predictions at various distances along a uniform second-order stream (similar to PKL) which flows from native bush into pasture. Shade factor 0.30, wind speed 1 m s-', humidity 90%, air temperature 10--20°C.

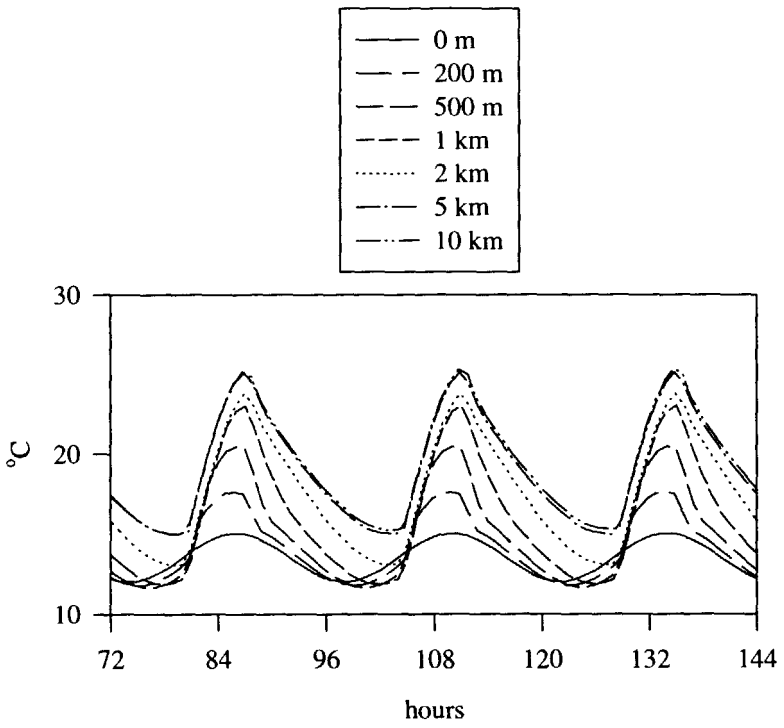

In first-order streams the daily maximum equilibrium temperature increases from 18ºC to 29ºC as shading decreases from 75% to 25% (Figure 41). As the amount of riparian shading decreases, more solar radiation reaches the stream and more heating occurs during the day. This behaviour is well documented in the literature (e.g., Brown 1969). It is also noticeable that the daily maximum equilibrium temperature decreases with increasing stream size: in the case of 25% shading from 29ºC in first-order streams to 24ºC in fifth-order streams. This reflects the fact that stream depth increases with increasing stream order (see Table 13) and that for the same flux of solar radiation across the water surface, the rate of change of temperature is inversely proportional to the water depth. The equilibrium temperature is reached more quickly in first-order than in the third- and fifth-order streams. This reflects the fact that the thermal inertia of small streams is low. Thus small, shallow streams are much more susceptible to heating as a result of the removal of riparian shade than are large, deep streams. Few first-order streams are more than about 1 km long but Fig. 41 indicates that daily maximum temperature increases of the order of 5ºC are possible in such streams when shade is reduced from 95% to 50% over 1 km. By comparison, temperature increases of 5ºC are only likely to occur in third- and fifth-order streams over distances of 10 and 20 km respectively, for comparable shade reductions. Figure 42 shows the predicted temperature decreases in streams which flow from an open (25% shaded) pasture channel into channels with 50%, 75%, and 95% shade. Initial temperatures were those predicted at equilibrium in pasture channels with 25% shade. Cooling occurs more rapidly in first-order than third- and fifth-order streams, again because the former are shallow and hence have low thermal inertia. In first-order streams, reductions in the daily maximum temperature of the order 5ºC are achievable over distances of about 1 km with restoration of dense (75%) shade. By comparison 5 and 12 km of dense (75%) shade are required to reduce temperatures by 5ºC in third- and fifth-order streams respectively. Regional differences in meteorological parameters (notably air temperature and solar radiation) will undoubtedly affect the absolute values of the predicted waters temperatures in Figs 41 and 42. Nevertheless, it is likely that the predicted changes in water temperature will be similar throughout New Zealand in streams like those described in Table 13 We conclude that in small, first-order streams, temperature changes of 5ºC can occur within 1–5 km while in deeper third- and fifth-order streams, not only are temperature changes smaller, but they occur over distances of 10–20 km.

The fact that the thermal inertia of small streams is low suggests that if low stream temperatures need to be maintained throughout a stream network (e.g., to maintain suitable fish or invertebrate habitat), then it is more important to maintain dense shade along the small (first- and second-order) than along the larger (third-, fourth- and fifth-order) streams. Similarly, when attempting to reduce stream temperatures in a catchment comprising a network of streams of different orders, it is more efficient to restore riparian shading on the shallow first- and second-order streams than on the deeper third-, fourth- and fifth-order streams.

Continue to next file: Streamshade03.pdf